Journal Pre-proof

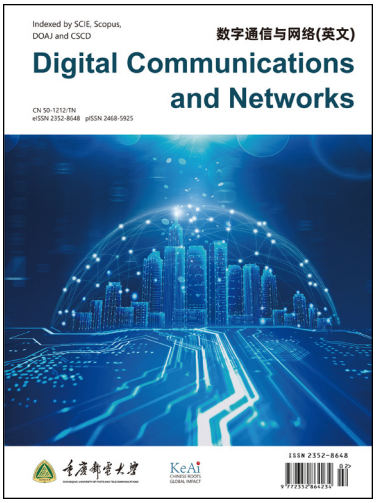

LOS and NLOS identification in real indoor environment using deep learning approach

Alicja Olejniczak, Olga Blaszkiewicz, Krzysztof K. Cwalina, Piotr Rajchowski and Jaroslaw Sadowski

PII: S2352-8648(23)00091-3
DOI: https://doi.org/10.1016/j.dcan.2023.05.009
Reference: DCAN 661

To appear in: *Digital Communications and Networks*

Received date: 11 May 2021
Revised date: 29 March 2023
Accepted date: 17 May 2023

Please cite this article as: A. Olejniczak, O. Blaszkiewicz, K.K. Cwalina et al., LOS and NLOS identification in real indoor environment using deep learning approach, *Digital Communications and Networks*, doi: https://doi.org/10.1016/j.dcan.2023.05.009.

Digital Communications and Networks(DCN)

Available online at www.sciencedirect.com

ScienceDirect

journal homepage: www.elsevier.com/locate/dcan

LOS and NLOS Identification in Real Indoor Environment Using Deep Learning Approach

Alicja Olejniczak*, Olga Blaszkiewicz, Krzysztof K. Cwalina, Piotr Rajchowski, Jaroslaw Sadowski

Faculty of Electronics, Telecommunications and Informatics, Gdansk University of Technology, Gdansk 80-233, Poland

Abstract

Visibility conditions between antennas, i.e. Line-of-Sight (LOS) and Non-Line-of-Sight (NLOS) can be crucial in the context of indoor localization, for which detecting the NLOS condition and further correcting constant position estimation errors or allocating resources can reduce the negative influence of multipath propagation on wireless communication and positioning. In this paper a deep learning (DL) model to classify LOS/NLOS condition while analyzing two Channel Impulse Response (CIR) parameters: Total Power (TP) [dBm] and First Path Power (FP) [dBm] is proposed. The experiments were conducted using DWM1000 DecaWave radio module based on measurements collected in a real indoor environment and the proposed architecture provides LOS/NLOS identification with an accuracy of more than 100% and 95% in static and dynamic senarios, respectively. The proposed model improves the classification rate by 2-5% compared to other machine learning (ML) methods proposed in the literature.

KEYWORDS:
Deep learning, Machine learning, LOS, NLOS, UWB

1. Introduction

Indoor environment attributes, especially multipath propagation, may significantly distort the transmitted signals, which is an important issue. Therefore, the most advanced concepts such as 5G, cyber-physical systems or the Internet of Things (IoT) are considered first, where the reliability of smart building systems is of strategic importance due to control, maintenance and security issues [1–3]. Hence, one of the possible methods to minimize errors determined by undesirable indoor environment influence to identify the direct undisturbed visibility conditions between antennas of communicating devices, i.e. Line-of-Sight (LOS) and Non-Line-of-Sight (NLOS) that occur when some obstacle blocks the direct path of transmission between the antennas, which may be crucial for the most common indoor services interconnecting a large number of distributed devices, localization, routing management and resources allocation [4–6].

Ultra Wide Band (UWB) technology can be considered as one of the most suitable solutions for indoor because its resistance to multipath effects and sub-meter distance measurement accuracy is determined by the wide bandwidth. Due to its wide bandwidth, UWB additionally provides high time resolution, which is essential in terms of indoor localization [7, 8]. Therefore, DecaWave DWM1000 UWB

*Alicja Olejniczak (Corresponding author), e-mail: alicja.olejniczak@pg.edu.pl
[1]Olga Blaszkiewicz, e-mail: olga.blaszkiewicz@pg.edu.pl
[2]Krzysztof K. Cwalina, e-mail: kkcwalina@eti.pg.edu.pl
[3]Piotr Rajchowski, e-mail: piorajch@eti.pg.edu.pl
[4]Jaroslaw Sadowski, e-mail: jaroslaw.sadowski@eti.pg.edu.pl

modules, compliant with IEEE 802.15.4-2015 standard, were chosen for the experiments presented in the given article.

The next issue is Artificial Intelligence (AI), which is becoming increasingly popular while considering the latest technologies, providing adaptability to changing environmental characteristics, and which is particularly effective for non-linear problems. Both machine learning (ML) and more complex deep learning (DL) methods have been found very useful recently, not only within strictly computer and automatic systems, but also in radiocommunication-related solutions, including networks management, localization, resource allocation, channel modelling or even receiving process as the support for classical error correction algorithms [9–11].

Taking the above into consideration a Deep Feedforward Neural Net (DFNN) architecture is presented to identify LOS and NLOS situations in real indoor environments using UWB signals. The proposed method can improve the position estimation or dynamic resource allocation in smart buildings, which is highly useful in terms of 5G or IoT systems.

In Section II, the current state of research on NLOS detection using ML method topics is reported, which will serve as a reference for further evaluation of the proposed model. In Section III, the measurement methodology and the characteristics of the collected data are described. In Section IV, the designed DFNN structure and its evaluation are presented. In the last section, conclusions are drawn and a short summary is given.

Article reference	Technology/ system	Type of research measurement static/ dynamic	ML method	Input parameters	Accuracy [%]
[20]	WiFi	static	Support Vector Machine (SVM)	5 Channel State Information (CSI) parameters	p_{mNLOS}: 18 p_{fNLOS}: 13
[21]	WiFi	static	SVM	Received Signal Strength Indicator (RSSI), 2 CSI parameters	overall: 94
[22]	WiFi	static and dynamic	Least Square SVM LS-SVM	3 Received Signal Strength (RSS) parameters	static: p_e: 6 dynamic: p_e: 12.5
[23]	UWB	static	SVM	6 Channel Impulse Response (CIR) parameters	p_{LOS}: 90.2 p_{NLOS}: 91.9
[24]	UWB	static	SVM	CIR	static 1: 92 static 2: 100
[25]	UWB	static	LS-SVM	3 CIR parameters	p_{mNLOS}: 9 p_{fNLOS}: 8.2
[26]	UWB	dynamic	Convolutional Neural Network	CIR	overall: 87.4
[27]	UWB	static	SVM	3 CIR parameters	overall: 93 p_{LOS}: 94.7 p_{NLOS}: 92.6
[28]	UWB	static	Logistic Regression	RSS, 8 CIR parameters	overall: 87.2 p_{LOS}: 87.8 p_{NLOS}: 86.5
[29]	UWB	static and dynamic	Multilayer Perceptron (MLP) and Boosted Decision Trees (BDT)	3 CIR parameters	static: 98 dynamic 1: MLP: 82, BDT: 87 dynamic2: MLP: 92, BDT: 94
[30]	Wireless Local Area Network (WLAN)	dynamic	Recurrent Neural Network	CSI and RSSI	overall: 91
[31]	Software Defined Radio (SDR)	static	Random Forest (RF)	4 CIR parameters	p_{LOS}: 96 p_{NLOS}: 98
Proposed solution	UWB	static and dynamic	DFNN	Total Power (TP) and First Path Power (FP)	static: p_{NLOS}: 100 p_{LOS}: 99.3 overall: 99.6 dynamic: p_{NLOS}: 92.1 p_{LOS}: 99.7 overall: 95.7

p_{LOS} - LOS accuracy, p_{NLOS} - NLOS accuracy, p_{mNLOS} - missed NLOS, p_{fNLOS} - false NLOS, $p_e = p_{mNLOS} + p_{fNLOS}$

Table 1 Articles describing ML-based LOS/NLOS identification

2. Related work

Since this paper deals with the application of ML in LOS/NLOS identification, it is a prerequisite to analyze the current research related to this topic. There are many articles that study this issue, some of which are systematized in Table 1. It is important to mention that, due to the specific interests of this topic, papers presenting only simulations or analytical solutions that do not involve ML or do not strictly deal with indoor environments (e.g., vehicle-to-vehicle communication, Global Navigation Satellite Systems, geolocation) are not more comprehensively described in the literature [12–19].

In Table 1, the most meaningful information is listed, such as the designed model and its input parameters, the technique or the best accuracy obtained. Whereas the presented literature mentions many different input features and parameters for validity assessment, all of them are listed in Table 1 in their original form and explained in the subsequent part of this paper.

Firstly, it is important to elaborate on the input parameters used in the above-mentioned methods. Because of the fact that some of the presented architectures are rather simple classifiers (e.g. SVM), the features extracted from CSI or CIR can be more appropriate as input parameters than the whole CSI or CIR itself, because mathematical structures, unlike DL, cannot express complex, nonlinear dependencies by itself. These features can be obtained directly from the signal and they are: the time of rise, the signal energy, the number of paths with more than 85% total energy, the power difference between the first and the strongest path, the amplitude, the Received Signal Power to the First Path Power level ratio (RFPR). And the others are quite statistical: skewness, Kurtosis, Rician K factor, mean, standard deviation, Mean Excess Delay (MED), or Root Mean Squared Delay Spread (RMS). Although all of these parameters occurred interchangeably in the literature and only specific sets of them are best for models performances, depending on the collected measurements and used architectures, they are not summarized in Table 1.

Secondly, the presented efficiency metrics should be explained. General accuracy, which indicates the ratio of the number of correct classifications to the total number of samples tested, is described overall. Analogically, LOS and NLOS accuracies (p_{LOS}, p_{NLOS}) equal the number of correct identifications of one of the conditions (LOS or NLOS) to the number of all its

samples. On the other hand, the other three parameters define the inaccuracy level as they pertain strictly to misclassifications occurring. p_{mNLOS} indicates the number of missed NLOS labels to the total number of all NLOS samples, and p_{fNLOS} defines false NLOS classifications, or simply missing LOS labels, out of the total number of LOS samples. p_e is the sum of p_{mNLOS} and p_{fNLOS} and it denotes the probability of error for the tested model. All these metrics will be further used in the proposed DFNN evaluation.

Analyzing the mentioned literature, it can be concluded that within all the articles at least 3 features are used as input parameters and the SVM model is evaluated in over half of them. Moreover, only four papers present an evaluation based on dynamic measurements and only one selected scenario has an accuracy of 94%. Since dynamic motion determines the occurrence of fast fading, it is important to include such scenarios during model evaluation and testing. An important issue is the assignment of data during the training and testing phases. Although in, e.g. [29], different scenarios are used for learning and testing, in [21, 24, 30] data from the same scenario is divided between the training and testing phases, which may impact the generality assessment of the designed model.

Considering the previously-mentioned methods, the use of ML methods to evaluate LOS/NLOS conditions can be very effective. However, the total accuracy depends strictly on the complexity of the tested model and the analyzed input parameters and it may vary significantly with respect to the measurement scenarios and the initial data. Thus, the goal of this paper was established – DL architecture for LOS/NLOS identification, with a stable accuracy of at least 94% for dynamic scenarios, taking into account real-time operation, with the smallest possible number of input values and directly available from the measurements. Additionally, it was decided to include fluent transitions between LOS and NLOS conditions in the measurement scenarios since the changeover issue has not been analyzed in the literature yet. The novelty of the proposed approach includes not only the usage of the promising AI-based models, but also their evaluation regarding different types of propagation conditions: static and dynamic scenarios involving dynamic, fluent changes between LOS and NLOS.

3. Experimental data collection

To meet the assumptions indicated in the previous section, it is important to choose the most suitable ML structure. Since the analyzed data included both static and dynamic measurements, a model handling the nonlinearity issue is needed. DFNN is the network that single-handedly distinguishes nonlinear dependencies based on an even highly reduced number of input parameters. At the same time, taking into account model complexity, it is still more suitable than a Recurrent Neural Network (RNN) or a Convolutional Neural Network (CNN). Before choosing a specific DFNN architecture for LOS/NLOS identification, data from the training and testing phases had to be collected in a real indoor environment. The measurements were performed during three separate campaigns: one static and two dynamic, at Gdansk University of Technology, using a UWB module: DecaWave DWM1000 working at 6489 MHz frequency and 499.2 MHz of bandwidth. During each scenario, two parameters were collected: Total Power (TP) [dBm] and First Path Power (FP) [dBm] based on CIR. Since CIR represents the system response to an input impulse signal, TP indicates the total received signal power (the sum of the power of all the components from a multipath propagation), and FP represents the power of the first received component. Both of them were read out from the node registers and then transmitted [32] with a repetition rate of 25 measurements per second to a data collector. A more comprehensive description of the measurement stand can be found in [33].

3.1. Campaigns 1 and 2

The first campaign (C1) is static and it consists of ten different scenarios: 1-6 are LOS, and 7-10 are NLOS scenarios, each containing approximately 8000 pairs of the collected CIR parameters. The second, dynamic campaign (C2) comprises nine scenarios: two LOS (approx. 7000 measurements for each) and seven NLOS (approx. 7000 measurements for each) scenarios. This gives over 140 000 TP and FP measurements. At first, all the NLOS scenarios were analyzed in terms of the distance dependency and then only two NLOS scenarios were chosen for further model evaluation to stick to an equal proportion of LOS/NLOS samples.

In Fig. 1 a plan view of the measurement area (typical classroom) for both campaigns, including the nodes arrangement and the movement trajectory, is presented. The collecting data node (blue dot) is placed in the centre of the room in the same spot for each campaign, while another node (green dots for LOS, and orange ones for NLOS) is moved between ten different measurement points for every single static scenario, and each node placement is marked with the corresponding scenario number. Both nodes are mounted on tripods and located approximately 1 m above the ground. Non-uniform distances between the consecutive points are determined by the room architecture (wall or pilasters). Additionally, the furniture such as desks or chairs is omitted in the given picture.

During the dynamic campaign (C2) the mobile node is moved by a person, back and forth along the trajectory denoted in Fig. 1 with solid lines (the green line for LOS and the red lines for NLOS) where each line represents a separate scenario. The movement speed of the node is a standard walking pace (approx. 1-1.2 mps). The node is moved at the same height as during

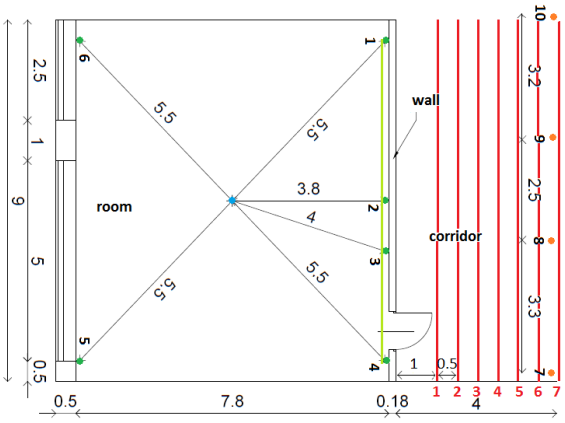

Fig. 1. C1 and C2 measurement plan view with dimensions in meters

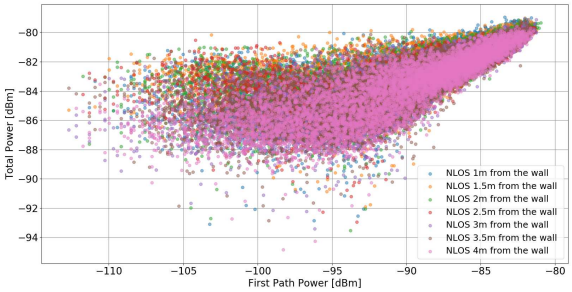

Fig. 2. Power parameters of measured data for mobile node at different distances (C2)

the static campaign (C1), i.e. 1 m above the ground.

Figures 2-3 show the results of the power parameter measurements, indicating their interdependence. In Fig. 2 the results for NLOS scenarios at different distances are shown, while in Fig. 3 (a) static and (b) dynamic campaigns with both LOS and NLOS variants are marked.

As long as the distance between the nodes does not affect the relation between TP and FP (Fig. 2), the edge values of the range (scenarios 1 and 7) are chosen for further analysis.

It can be observed that the dynamic scenarios (Fig. 3) are characterised by sparser power values than the static ones (Fig. 2). Additionally, for the dynamic scenarios both LOS and NLOS data points are overlapping, which impedes the identification process. This proves that the analysis of the data collected during the dynamic measurements is crucial for designing a holistic classification model.

It is important to mention that apart from the measurement dynamics, electric parameters of the obstacles also influence the collected data. During the 7th scenario from the static campaign (C1), the nodes communicate through a glass door and in this case sparser power values can be discerned, i.e. FP: 15.8 dB, TP: 9.2 dB dispersion for 7th scenario (C1) and FP: 33.1 dB, TP: 11.6 dB dispersion for 3rd scenario (C2). Dispersion is defined as the difference between the minimum and maximum received power values.

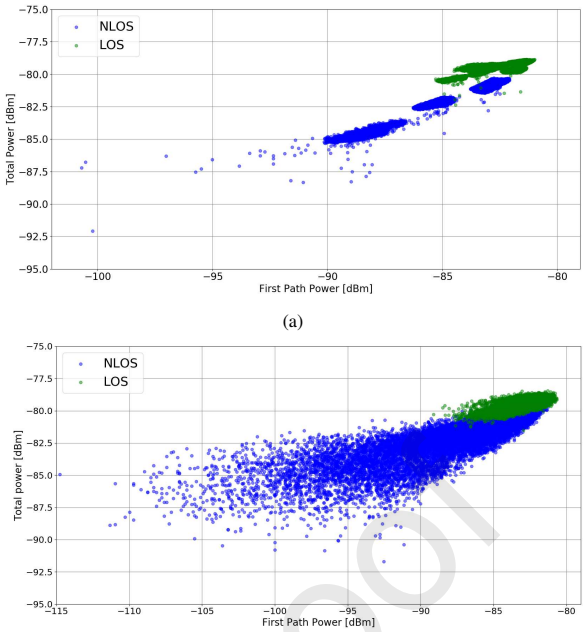

Fig. 3. Power parameters of measured data (a) TP(FP) for C1 (b) TP(FP) for C2

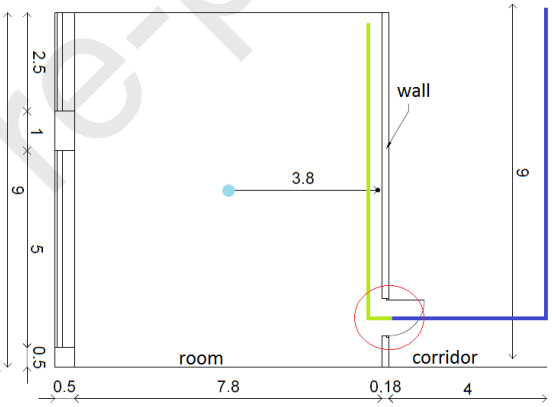

Fig. 4. C3 measurement plan view with dimensions in meters

3.2. *Campaign 3*

The third campaign (C3) is also dynamic and it consists of twenty different scenarios, each with approximately 700 measurements. It is conducted in a different room, but with the same structure. In Fig. 4 the plan view with a movement trajectory is presented: a dark blue line for NLOS and a light green for LOS condition. The reference node position is unchanged (a blue dot).

It can be noticed that in this case both LOS and NLOS are present in each scenario. To properly label the data and find the exact transition between LOS and NLOS (marked with a red circle) an algorithm for object recognition was applied [34]. The application using a USB camera (mounted on the reference node) sends '1' (LOS information) to the reference node each time it recognizes the symbol located on the measurement node, and '0' otherwise.

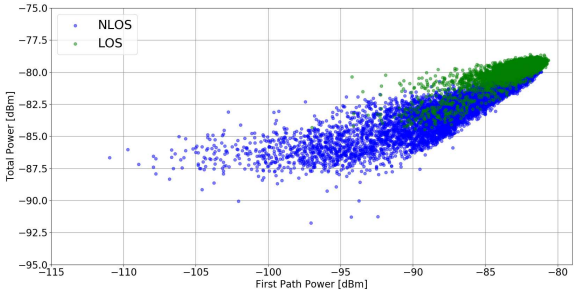

Fig. 5. Power parameters of measured data TP(FP) for C3

The applied image recognition algorithm is the Haar cascade of classifiers, proposed in [34]. The cascade function is trained by the sets of positive (containing the recognized object) and negative (containing only backgrounds) images, from which distinctive features with the corresponding sums of pixels are extracted. For object recognition, the most effective features are selected by the meta-algorithm AdaBoost [35].

The highest dispersion for this campaign equals 30.2 dB for FP and 12.4 dB for TP. The dependence of those power parameters for all the scenarios with the distinguished LOS and NLOS conditions is presented in Fig. 5.

All the presented power parameter values are initial features used in further DFNN evaluation. Before forwarding them into the network, they were normalized to [0,1] range, to improve the performance of the model convergence based on possible min/max values that can be estimated by DW1000 radio module in the real scenario. Simply speaking, the TP and FP values are normalized and then treated as the DFNN input. Based on such input data, network classifies the current visibility condition as LOS or NLOS. Additionally, the presented campaigns data are not merged, i.e. the measurements for the learning phase are derived from a different campaign than those used in the testing phase. There are two main reasons for separating the static, dynamic and dynamic with smooth LOS/NLOS transition datasets during the training and testing phases. Firstly, it allows for analyzing the robustness of a given solution and to evaluate the accuracy of the LOS/NLOS classification for measurement data of different nature. Better generalization leads to the second aspect, namely the control of the overfitting problem.

4. Results and discussion

Collecting the measurement data allowed for designing the optimal neural network architecture and evaluating the performance of LOS/NLOS identification. This process is divided into two subsections. In the first section, the modeling process of DFNN is introduced, including describing the general network operations and determining the final structure. In the second part, the final results are presented and compared with the other two methods.

4.1. Network modelling

In Fig. 6 the proposed DFNN architecture with the marked connections between the nodes across all the layers is shown. A simpler version of the presented structure is previously introduced in [36]. $\{n_{l,1}, n_{l,2}, n_{l,3}, ..., n_{l,i}\}$ represent each node $\{1, ..., i\}$ within l layer. The output y for the exemplary first node in the first hidden layer can be described by the following formula:

$$y_1 = f(\sum_{j=1}^{i} x_j w_j + b_1) \tag{1}$$

where $\{x_1, x_2, x_3, ..., x_j\}$ indicate input parameters, and w_j for $j = 1, 2, \ldots$ represents node weights. The additional bias weight is denoted as b_n, where $n = 1, 2, 3$ and the activation function is $f()$.

The final output denoted as n_{out1} and n_{out2} is calculated based on the logSoftmax activation function which yields normalized values representing probability, including the given input and the two examined classes: LOS and NLOS.

During the learning process, all weights are modified in order to minimize the difference between the network output and the reference output. The level of such a weight modification will be further described as the learning rate. Considering the popularity of the neural networks and numerous publications providing an extensive description of the mathematical background regarding the presented architecture, a more detailed explanation can be found in [37, 38].

The presented structure is the final model that is selected using a grid search based on C3, i.e. the most complex data, in terms of both the measurement methodology and the obtained power parameters (Fig. 5), as a learning set, and C2 as a testing set. The grid search method examines all the potential model structures based on a given set of possible parameters. Although this method can be considered redundant (for more complex identification problems genetic algorithms can be more efficient) for that type of classification, it proved sufficient. The set of (1-4) hidden layers is evaluated, with varying activation functions (Sigmoid and ReLU) and batch sizes (1-150). All the models are trained for a fixed learning rate equal to 0.001 and converged below 100 epochs. Based on the performed parameter search, architectures with 3 or more hidden layers provide considerable validity, so that the set of layers 1-4 is not further extended. Following across-the-board parameter search, only the final result of the extraction is presented. The evaluated model represents the best trade-off between the identification efficiency and the lowest model complexity.

The architecture details, strictly pertaining to the learning process (e.g. to the activation function for each hidden layer), are systematized in Table 2

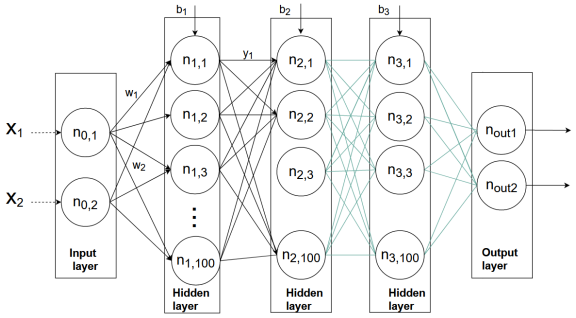

Fig. 6. Proposed DFNN architecture

Layer, No. of nodes	Activation function
1, 100	Rectified Linear Unit (ReLU)
2, 100	ReLU
3, 100	ReLU
No. of epochs	50
No. of batches	150
Learning rate	0.001
Optimization algorithm	Adaptive Moment Estimation (ADAM)

Table 2 DFFN architecture parameters

The epochs number indicates the optimal quantity of iterations during the training phase, and the number of batches represents the sets of a few different samples from the learning data collection. ADAM is chosen as an optimization algorithm that is applied to dynamically varying learning rate parameters during the updating of weights. It allows to improve the effectiveness of model convergence [39].

4.2. DFNN evaluation and final results

Since the architecture of the DFNN has been determined, it is possible to verify the validity of the classification performance. For comparison, the learning and testing process also used the algorithms mentioned in Section 1, i.e., SVM with linear and Radial Basis Function (RBF) kernels, and RF [20, 31].

Considering the character of the collected data, only dynamic campaigns are included in the learning process during the proposed DFNN model evaluation. Moreover, randomness of the initial weights and shuffling data samples during separate tests determine limited repeatability of separate learning processes and the variability of the final results. Hence, only the best final results (extracted from the 10 individual trials of each configuration) are presented in Table 3.

The above results show that the proposed DFNN structure outperforms the other methods regarding three different variants: C2/C1, C2/C3 and C3/C2 by about 2% compared with the second best method and from 5% to 10% compared with the worst evaluated algorithm. In the case of C3/C1, all the methods offered over 99% accuracy. Moreover, DFNN yielded the highest mean values for particular p_{NLOS} and p_{LOS} metrics, i.e. 97.5% and 97.2% respectively. The second best structure, SVM with RBF kernel, resulted in

Architecture	Training set	Testing set	p_{NLOS} [%]	p_{LOS} [%]	Accuracy [%]
DFNN	C2	C1	100	99.32	**99.60**
	C2	C3	97.91	89.88	**94.01**
	C3	C1	100	99.95	**99.97**
	C3	C2	92.08	99.72	**95.74**
	Mean value:		**97.50**	**97.22**	**97.33**
Linear SVM	C2	C1	100	83.15	**90.03**
	C2	C3	99.07	84.00	**91.75**
	C3	C1	98.03	99.98	**99.18**
	C3	C2	81.47	99.98	**90.33**
	Mean value:		**94.64**	**91.78**	**92.82**
RBF SVM	C2	C1	100	96.18	**97.74**
	C2	C3	99.43	83.23	**91.56**
	C3	C1	99.97	99.98	**99.98**
	C3	C2	87.75	99.96	**93.60**
	Mean value:		**96.79**	**94.84**	**95.72**
RF	C2	C1	100	84.77	**90.99**
	C2	C3	99.48	78.36	**89.21**
	C3	C1	98.88	99.92	**99.49**
	C3	C2	86.53	99.91	**92.94**
	Mean value:		**96.22**	**90.74**	**93.16**

Table 3 Overall accuracy results

p_{NLOS} equal to 96.8% and p_{LOS} equal to 94.8%. Although the results for static C1 dataset identification for both DFNN and SVM with RBF can be comparable, it should be noted that DFNN presents noticeably higher effectiveness in the case of dynamic measurement data analysis, i.e. C2 and C3 testing datasets. The dynamic character of the collected data, due to the occurrence of fast fading, determines data nonlinearity. Thus, the DFNN-based solution surpasses all the other evaluated methods. It is also worth mentioning that the proposed DFNN model is proved to be the most stable one: the difference between the best and the worst result (marked with the red colour) for each method equaled: 5.6%, 8.4%, 9.2% and 10.3% for DFNN, RBF SVM, Linear SVM and RF respectively.

Considering a given accuracy rate, it also occurs that, apart from the 99% accuracy rate, the tested models provide nonsymmetric identification performance, where one condition is classified much better than the other. This stems from the specificity of the learning process, i.e., the mathematical structure is more suitable for one of the LOS/NLOS variants.

Additionally, influence of the chosen training dataset on the final identification efficiency can be discerned. The DFNN accuracy of C2 as training set and C3 as test set is expected to be lower (94%) than that of the swap set (95%), since C3 movement trajectory is more complex (with LOS/NLOS transition). These results suggest that even some brief dynamic scenarios containing LOS/NLOS transformations may be sufficient to train the proposed model for use in new real-world operational environments.

In Fig. 7-10 false detection rates for each training/testing variant and each model are presented. They represent the p_{mNLOS} and p_{fNLOS} which are defined in section 2. It can be observed that the model learns better for one of the variants (LOS or NLOS) provides more false detection for this variant, and less for the other one. Thus, as long as one of the accuracies equals 100% for each algorithm (Tab. 3), only one colour is displayed on the bar (Fig. 7).

Analyzing the given bar plots, it can be noticed that

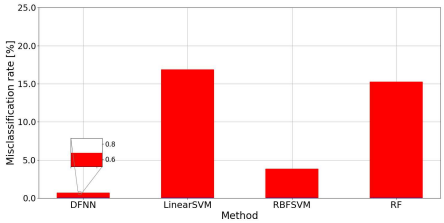

Fig. 7. Misclassification rate for C2 (training) C1 (testing) sets

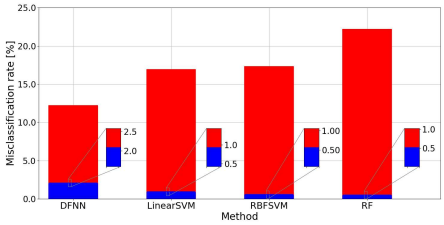

Fig. 8. Misclassification rate for C2 (training) C3 (testing) sets

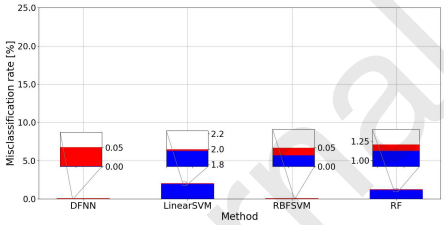

Fig. 9. Misclassification rate for C3 (training) C1 (testing) sets

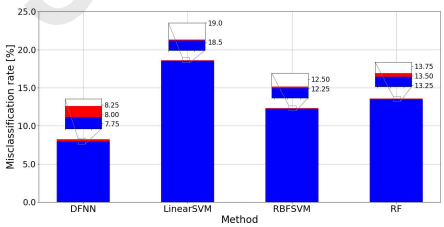

Fig. 10. Misclassification rate for C3 (training) C2 (testing) sets

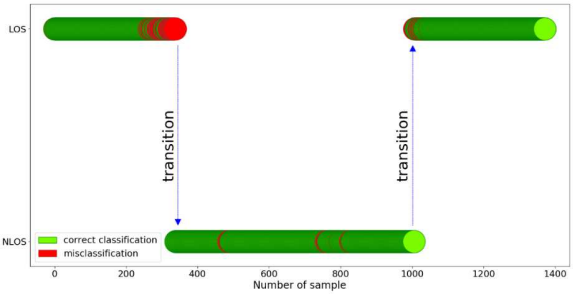

Fig. 11. Misclassifications within exemplary scenarios (C2/C3)

each training dataset (C2 and C3) determines different learning performance, not only with reference to the final accuracy, but also with respect to the better adaptation of the model to a specific direct visibility condition. Hence, for C2 training dataset more false NLOS classifications occurres, while for C3 training dataset misclassifications are mostly based on the missed NLOS cases.

The last step of analyzing the obtained results is to evaluate the areas (in the environmental context) where misclassifications appear. Nevertheless, since the collected data contain power measurements and LOS/NLOS labels only, the explicit node position corresponding to the error occurrence cannot be indicated. Thus, in Figure 11, exemplary misclassifications are presented with reference to the LOS/NLOS changeover as a function of samples.

It can be noticed that the identification errors of DFNN occur especially in the transition regions, especially the LOS to NLOS transition. However, some misclassifications also occur in the stable NLOS region (dark blue line in Fig. 4). The authors suggest that augmenting the collected data with more time-dependent information may reduce the above misclassification problem. Nevertheless, such research remains in future plans.

5. Conclusions

The given paper substantiates the validity of using ML methods in terms of classifying the LOS/NLOS problem within the real indoor environment. The presented research showes that the optimal DFNN architecture may allow proper identification of the direct visibility conditions. Even if the input parameters characterizing the communication environment are reduced to only two components instead of, e.g. the whole CIR, it still outperforms state-of-the-art methods presented in section 2. Moreover, the designed training and testing structure, which utilizes separate measurement data obtained during different campaigns, still provides the LOS/NLOS classification with 95% accuracy for a dynamic environment, and over 99% for a static one.

The particular case study presented in the paper can be used within indoor systems in both localization, as

a tool to reduce the position estimation error, and in other radiocommunication-related systems, e.g. for routing optimization or resource allocation. Considering the potential applications of such solutions in real radiocommunication systems, the most critical factors that should be considered are undoubtedly time and computational complexity.

Since the proposed decision-making process is based on single FP and TP values (directly read from DWM1000 radio modem register) only, the real-time operation is possible. This is an important advantage of DFNN (or any simpler ML method) in comparison to ML models analyzing also time-dependent changes, e.g. Long Short-Term Memory or RNN. Although such architectures may be more suitable in the case of dynamics of the measurement methodology, which significantly affects the identification process because of additional issues occurring during the node motion (e.g. fast fading), they also require historical input values for efficient classification.

Regarding the computational complexity there are various, more basic ML methods that outperform deep learning, such as SVM. Nevertheless, the results presented in the paper have shown that those less complex models provide similar accuracy only for static measurement scenarios. In the case of a dynamic environment, it is still more reasonable to use the DFNN model. Considering the fact that the proposed deep architecture is rather simple (3 layers, ReLU activation function), it is possible to provide a LOS/NLOS classification based on TP and FP values within the measurement time resolution (40 ms), even on a microcontroller with low computational power. Thus, the proposed model may be implemented inside both fixed network infrastructure and individual nodes.

Undeniably, additional testing of the above-shown DFNN structure is still needed. The presented model should be evaluated and extended to cover different areas and obstacles determining the NLOS state (e.g. different buildings, types of wall, furniture, people) which directly affects the estimated CIR. Furthermore, it would be valuable to analyze the relation between the collected data characteristics and the final results of accuracy to derive the set of data which is most effective during the learning process. Finally, more deep learning-based structures can be analyzed and compared, including both time-dependent and time-independent models.

Acknowledgements

This work was supported under ministry subsidy for research for Gdansk University of Technology.

Data availability

Datasets used in this research are available for free from the authors with the CC BY license.

References

[1] F. Kirsch, R. Miesen, M. Vossiek, Precise local-positioning for autonomous situation awareness in the Internet of Things, IEEE MTT-S International Microwave Symposium Digest (2014). doi:10.1109/MWSYM.2014.6848674.

[2] Y. Zhong, E. Dutkiewicz, Y. Yang, X. Zhu, Z. Zhou, T. Jiang, Internet of mission-critical things: human and animal classification-a device-free sensing approach, IEEE Internet of Things Journal 5 (5) (2018) 3369–3377. doi:10.1109/JIOT.2017.2760322.

[3] A. A. Adebomehin, S. D. Walker, Impulse radio Ultrawideband D2D-based localization for ultra-dense 5G networks, 2017 IEEE 18th Wireless and Microwave Technology Conference, WAMICON 2017 (2017). doi:10.1109/WAMICON.2017.7930262.

[4] Pinky, A. Pandey, S. Kumar, Smart device localization using femtocell and macro base station based path loss models in IoT networks, International Symposium on Advanced Networks and Telecommunication Systems, ANTS (2019) 1–6doi:10.1109/ANTS.2018.8710150.

[5] W. Wang, S. L. Capitaneanu, D. Marinca, E.-S. Lohan, Comparative analysis of channel models for industrial IoT wireless communication, IEEE Access 7 (2019) 91627–91640. doi:10.1109/access.2019.2927217.

[6] G. P. Koudouridis, C. Qvarfordt, A method for the generation of radio signal coverage maps for dense networks, IEEE International Conference on Communications 2018-May (2018) 1–6. doi:10.1109/ICC.2018.8422495.

[7] D. Dardari, N. Decarli, A. Guerra, F. Guidi, The future of ultra-wideband localization in RFID, 2016 IEEE International Conference on RFID, RFID 2016 (2016). doi:10.1109/RFID.2016.7487998.

[8] D. Dardari, A. Conti, U. Ferner, A. Giorgetti, M. Z. Win, Ranging with ultrawide bandwidth signals in multipath environments, Proceedings of the IEEE 97 (2) (2009) 404–425. doi:10.1109/JPROC.2008.2008846.

[9] A. M. Bosneag, M. X. Wang, Intelligent network management mechanisms as a step towards SG, Proceedings of the 2017 8th International Conference on the Network of the Future, NOF 2017 2018-Janua (2018) 52–57. doi:10.1109/NOF.2017.8251220.

[10] Z. M. Fadlullah, F. Tang, B. Mao, N. Kato, O. Akashi, T. Inoue, K. Mizutani, State-of-the-art deep learning: evolving machine intelligence toward tomorrow's intelligent network traffic control systems, IEEE Communications Surveys and Tutorials 19 (4) (2017) 2432–2455. doi:10.1109/COMST.2017.2707140.

[11] Q. Mao, F. Hu, Q. Hao, Deep learning for intelligent wireless networks: A comprehensive survey, IEEE Communications Surveys and Tutorials 20 (4) (2018) 2595–2621. doi:10.1109/COMST.2018.2846401.

[12] F. Lyu, N. Cheng, H. Zhu, H. Zhou, W. Xu, M. Li, X. S. Shen, Intelligent context-aware communication paradigm design for IoVs based on data analytics, IEEE Network 32 (6) (2018) 74–82. doi:10.1109/MNET.2018.1800067.

[13] F. Lyu, N. Cheng, H. Zhou, W. Xu, W. Shi, J. Chen, M. Li, DBCC: leveraging link perception for distributed beacon congestion control in VANETs, IEEE Internet of Things Journal 5 (6) (2018) 4237–4249. doi:10.1109/JIOT.2018.2844826.

[14] B. Guermah, H. El Ghazi, T. Sadiki, H. Guermah, A robust GNSS LOS/Multipath signal classifier based on the fusion of information and machine learning for intelligent transportation systems, in: 2018 IEEE International Conference on Technology Management, Operations and Decisions, ICTMOD 2018, IEEE, 2019, pp. 94–100. doi:10.1109/ITMC.2018.8691272.

[15] L. T. Hsu, GNSS multipath detection using a machine learning approach, IEEE Conference on Intelligent Transportation Systems, Proceedings, ITSC 2018-March (2018) 1–6. doi:10.1109/ITSC.2017.8317700.

[16] B. Chitambira, S. Armour, S. Wales, M. Beach, NLOS identification and mitigation for geolocation using least-squares support vector machines, IEEE Wireless Commu-

nications and Networking Conference, WCNC (2017) 1–6doi:10.1109/WCNC.2017.7925566.

[17] V. H. Nguyen, M. T. Nguyen, J. Choi, Y. H. Kim, NLOS identification in WLANs using deep LSTM with CNN features, Sensors (Switzerland) 18 (11) (2018) 1–13. doi:10.3390/s18114057.

[18] J. Fan, A. S. Awan, Non-line-of-sight identification based on unsupervised machine learning in ultra wideband systems, IEEE Access 7 (2019) 32464–32471. doi:10.1109/ACCESS.2019.2903236.

[19] G. Ding, Z. Tan, J. Wu, J. Zhang, Efficient indoor fingerprinting localization technique using regional propagation model, IEICE Transactions on Communications E97-B (8) (2014) 1728–1741. doi:10.1587/transcom.E97.B.1728.

[20] X. Cai, X. Li, R. Yuan, Y. Hei, Identification and mitigation of NLOS based on channel state information for indoor WiFi localization, 2015 International Conference on Wireless Communications and Signal Processing, WCSP 2015 (2015) 1–5doi:10.1109/WCSP.2015.7341172.

[21] X. Li, X. Cai, Y. Hei, R. Yuan, NLOS identification and mitigation based on channel state information for indoor WiFi localisation, IET Communications 11 (4) (2017) 531–537. doi:10.1049/iet-com.2016.0562.

[22] Z. Xiao, H. Wen, A. Markham, N. Trigoni, P. Blunsom, J. Frolik, Non-line-of-sight identification and mitigation using received signal strength, IEEE Transactions on Wireless Communications 14 (3) (2015) 1689–1702. doi:10.1109/TWC.2014.2372341.

[23] Z. Zeng, S. Liu, L. Wang, UWB NLOS identification with feature combination selection based on genetic algorithm, 2019 IEEE International Conference on Consumer Electronics, ICCE 2019 (2019) 1–5doi:10.1109/ICCE.2019.8662065.

[24] J. B. Kristensen, M. M. Ginard, O. K. Jensen, M. Shen, Non-line-of-sight identification for UWB indoor positioning systems using support vector machines, 2019 IEEE MTT-S International Wireless Symposium (IWS) (2019) 1–3.

[25] S. Maranò, W. M. Gifford, H. Wymeersch, M. Z. Win, NLOS identification and mitigation for localization based on UWB experimental data, IEEE Journal on Selected Areas in Communications 28 (7) (2010) 1026–1035. doi:10.1109/JSAC.2010.100907.

[26] K. Bregar, M. Mohorcic, Improving indoor localization using convolutional neural networks on computationally restricted devices, IEEE Access 6 (2018) 17429–17441. doi:10.1109/ACCESS.2018.2817800.

[27] M. Kolakowski, J. Modelski, Detection of direct path component absence in NLOS UWB channel, MIKON 2018 - 22nd International Microwave and Radar Conference (2018) 247–250doi:10.23919/MIKON.2018.8405190.

[28] R. Zandian, U. Witkowski, Differential NLOS error detection in UWB-based localization systems using logistic regression, 2018 15th Workshop on Positioning, Navigation and Communications, WPNC 2018 (2018) 1–6doi:10.1109/WPNC.2018.8555750.

[29] S. Krishnan, R. Xenia Mendoza Santos, E. Ranier Yap, M. Thu Zin, Improving UWB based indoor positioning in industrial environments through machine learning, 2018 15th International Conference on Control, Automation, Robotics and Vision, ICARCV 2018 138632 (65) (2018) 1484–1488. doi:10.1109/ICARCV.2018.8581305.

[30] J. S. Choi, W. H. Lee, J. H. Lee, J. H. Lee, S. C. Kim, Deep Learning based NLOS identification with commodity WLAN devices, IEEE Transactions on Vehicular Technology 67 (4) (2018) 3295–3303. doi:10.1109/TVT.2017.2780121.

[31] M. Ramadan, V. Sark, J. Gutiérrez, E. Grass, NLOS identification for indoor localization using random forest algorithm, WSA 2018; 22nd International ITG Workshop on Smart Antennas (February) (2018) 1–5.

[32] DecaWave, DWM1000 User Manual, v.2.09 (2016).

[33] K. K. Cwalina, S. J. Ambroziak, P. Rajchowski, An off-body narrowband and ultra-wide band channel model for body area networks in a ferryboat environment, Applied Sciences (Switzerland) 8 (6) (2018) 1–16. doi:10.3390/app8060988.

[34] P. Viola, M. Jones, Rapid object detection using a boosted cascade of simple features, in: Proceedings of the IEEE Computer Society Conference on Computer Vision and Pattern Recognition, Kauai, USA, 2001. doi:10.1109/cvpr.2001.990517.

[35] Y. Freund, R. E. Schapire, A short introduction to Boosting 14 (5) (2015) 771–780. arXiv:1508.01136.
URL http://arxiv.org/abs/1508.01136

[36] K. K. Cwalina, P. Rajchowski, O. Blaszkiewicz, A. Olejniczak, Deep learning-based LOS and NLOS identification in wireless body area networks, MDPI Sensors 19(19) (4229) (2019).

[37] I. Goodfellow, Y. Bengio, A. Courville, Deep Learning, MIT Press, London, 2016.

[38] J. Patterson, A. Gibson, Deep Learning a Practitioner's Approach, O'Reilly, USA, 2017.

[39] D. P. Kingma, J. L. Ba, ADAM: A Method for Stochastic Optimization (2014) 1–15arXiv:arXiv:1412.6980v9.

Declaration of interests

☒ The authors declare that they have no known competing financial interests or personal relationships that could have appeared to influence the work reported in this paper.

☐The authors declare the following financial interests/personal relationships which may be considered as potential competing interests: